

Adaptations during cognitive control involve theta oscillations within trials and beta oscillations across trials in both the human prefrontal cortex and subthalamic nucleus

Baltazar Zavala¹, Anthony Jang¹, Michael Trotta¹, Codrin I. Lungu², Peter Brown³, and Kareem A. Zaghloul¹ [†]

¹ Surgical Neurology Branch, NINDS, National Institutes of Health, Bethesda, MD 20892, USA

² Division of Clinical Research, NINDS, National Institutes of Health, Rockville, MD 20852, USA

³ Medical Research Council Brain Network Dynamics Unit at the University of Oxford and Nuffield Department of Clinical Neurology, University of Oxford, John Radcliffe Hospital, Oxford, OX3 9DU, United Kingdom

Draft Date: March 12, 2018

Number of Figures: 7

Acknowledgements: This work was supported by the Intramural Research Program of the National Institute for Neurological Disorders and Stroke. PB was supported by the Medical Research Council (MC_UU_12024/1). We are indebted to all patients who have selflessly volunteered their time to participate in this study.

The authors declare no competing financial interests.

Author Contributions: B.Z. and K.Z. designed the research and analyzed the data. B.Z., A.J., M.T., C.L., P.B., and K.Z. performed the research and wrote the paper.

[†]Correspondence should be addressed to:

Kareem A. Zaghloul

Surgical Neurology Branch, NINDS, National Institutes of Health Building 10, Room 3D20
10 Center Drive Bethesda, MD 20892-1414

Office: (301) 496-2921

Email: kareem.zaghloul@nih.gov

Abstract

The medial prefrontal cortex (mPFC) participates in conflict and feedback monitoring while the subthalamic nucleus (STN) adjusts actions, yet how these structures coordinate their activity during cognitive control remains poorly understood. We recorded from the human mPFC and STN during a novel response inhibition task involving cognitive control both within and across trials. Within-trial adaptations to conflict involved theta band activity. Yet despite conflict related increases in mPFC-STN theta phase synchrony, mPFC theta power reflected early response inhibition while STN theta power reflected later response execution. Across-trial adaptations to both conflict and errors involved beta band activity. Yet conflict and errors modulated mPFC beta power immediately following each response and modulated STN beta power only during the subsequent trial. Our data therefore demonstrate that the complementary roles of the mPFC and STN, rather than the specific frequencies themselves, govern the behavioral correlates of oscillatory activity during cognitive control.

Introduction

To successfully navigate a complex and rapidly changing world, we must continually monitor and adjust our actions due to conflicts, mistakes, and negative feedback. This ability is referred to as cognitive control, and involves several separate yet related processes that together optimize goal-directed behavior (1, 2, 3). Cognitive control is necessary, for instance, in situations that require overcoming a habitual movement when selecting the most appropriate action among multiple conflicting choices (1). For example, when crossing the street, individuals from most countries will habitually first look for cars coming from the left, and then the right, before committing to crossing the street. However, when these individuals are crossing a street in the United Kingdom for the first time, they may abruptly find that they actually need to first look to the right. Cognitive control involves not only monitoring for such instances that require altering a pre-potent action, but also adapting to the current environment so as to appropriately adjust future actions. When approaching the next street, the same individuals may now consciously make an effort to look to the right first so as not to repeat the same mistake.

Cognitive control has been largely thought to involve structures of the medial prefrontal cortex (mPFC) (3). Neural activity within the mPFC has been linked with conflict monitoring during tasks in which individuals must either decide between multiple competing actions or suppress pre-potent automatic actions in favor of slower, more goal directed ones (1, 4, 5, 6). During both conflict and error trials, neural activity within the mPFC increases, and these increases correlate with slower response times on the current trial and on subsequent trials (7, 8, 9, 10, 11, 12). The ability to adjust these response times following error or conflict is impaired in both humans and rodents with lesions of the mPFC (13, 10, 14).

Recent evidence, however, has suggested that the subthalamic nucleus (STN) may also participate in cognitive control (15). The STN receives afferent connections from cortical regions involved in cognitive control (16, 17, 18), and projects efferent connections to other basal ganglia structures involved in movement inhibition (19, 20). Beta oscillations (10-30 Hz) within the STN regulate both motor and non-motor actions and increase when individuals must cancel or slow down a pre-planned action (21, 22, 23, 24, 25, 26, 27, 28, 29). Theta oscillations (2-8 Hz) and spiking activity in the STN also increase when individuals are making decisions in the presence of conflict (30, 31, 15, 32), and importantly, these conflict-related increases in theta oscillations are coherent with theta activity in the mPFC (31, 32). Furthermore, high frequency deep brain stimulation (DBS) of the STN appears to disrupt this mPFC-STN network, consequently leading to more conflict related errors (33, 4), although low frequency DBS may have potential benefits for response inhibition (18). These anatomical and functional links between the mPFC and the STN therefore suggest that the two structures may intimately interact to mediate cognitive control. Yet in what ways the roles of these two brain regions may or may not be complementary, remains unclear.

One possibility is that the STN and mPFC form a hierarchical relationship in the context of cognitive processing. The mPFC has been implicated in determining which actions and strategies are most appropriate in a changing environment (1, 34, 35). Monitoring for errors and adjusting to a changing set of task rules would require the higher order level of cognitive control afforded by the mPFC, focused in this case on continuously selecting the most optimal strategy or set of actions for the behavioral task at hand. Conversely, the STN is directly involved in the execution

of actions (36, 37). Cognitive control as implemented by the STN therefore may reflect the ability to defer a response so that the most appropriate action may be achieved among competing choices and under different time pressures.

It seems reasonable therefore to ascribe different, albeit overlapping and complementary, roles to these two coupled structures. But how are these roles subserved by changes in the activities of neurons and local populations of neurons? Specifically, can these roles be mapped on to the classical distinction between cognitive-theta and motoric-beta activities, or is the coordination of processing more nuanced? We explore these questions here by examining changes in neural activity in both the human STN and mPFC while participants perform a novel response inhibition task. We were specifically interested in how complementary activity within the STN and mPFC reflects cognitive control related to both the execution of a current action and the adjustments that are made for future actions. Using intra-operative microelectrode and subdural recordings captured during DBS surgery, we examine simultaneous oscillatory activity from the STN and the mPFC and find a temporally sequenced, spatio-spectral segregation in the pattern of neural activity. Theta activity increases in both regions to adjust the current action during conflict, but theta increases in the mPFC and the STN seem to be involved during separate portions of the task. Beta activity, on the other hand, although also present at both sites, exhibits opposing behavior between the two regions. In the STN, beta activity primarily decreases and is involved in the direct control of gating a movement, whereas in the mPFC beta activity primarily increases and is involved in adaptations that occur as a result of error or conflict. Taken together, our results evidence the basic principle that the precise behavioral associations of oscillatory activity are determined not by frequency band per se, but by the circuits in which they are expressed.

Results

22 participants (19 males; 58.0 ± 1.5 (mean \pm SEM) years old) undergoing DBS surgery for Parkinson’s disease performed a novel response inhibition task involving three different trial types (Fig. 1a; 34 total experimental sessions; see Materials and Methods). On each trial, participants attended to a centrally located arrow and moved a joystick in response. They were instructed to move in the direction of the arrow if the arrow was blue (Go) or move in the opposite direction if the arrow was red (Conflict). The ratio of Go:Conflict trials was 3:1. In a subset of trials, the arrow was presented surrounded by a white border, in which case the participants were instructed to withhold their response (NoGo). These trials served as an important control that enabled us to dissociate movement from difficulty by making two critical distinctions: a distinction between difficult (Conflict) and easy (Go and NoGo) trials independent of movement, and a distinction between movement (Go and Conflict) and no-movement (NoGo) trials independent of difficulty.

These distinctions were justified by the behavioral responses of the participants (Fig. 1b). Overall, participants made errors on $2.3\% \pm 0.4$ of the Go trials and $3.2\% \pm 0.7$ of the NoGo trials, but on $11.6\% \pm 2.1$ of the Conflict trials (ANOVA, within subjects repeated measures, $F(2, 33) = 21.35$, $p < 0.001$). The more difficult Conflict trials showed significantly higher error rates than the easier Go ($t(33) = 4.82$, $p < 0.05$, post hoc t -test) and the NoGo trials ($t(33) = 4.62$, $p < 0.05$, post hoc t -test). The Go and the NoGo trials showed no significant difference in error rates ($t(33) = 1.59$, $p > 0.05$, post hoc t -test). Correct Conflict trials also had significantly longer response times than correct Go trials across experimental sessions (963.8 ± 17.1 ms versus 831.5 ± 17.2 ms; $t(33) = 15.18$, $p < 0.001$, paired t -test). The difference in response times between Conflict and Go trials was robust at the individual session level. In 32 of the 34 experimental sessions, response times were significantly slower during the Conflict condition ($p < 0.05$, within session unpaired t -test).

Notably, participants adjusted and slowed their behavioral responses following correct trials that involved Conflict and following trials that in which the participant committed an error. Response times during correct Go trials that followed a correct Conflict trial were 139.0 ± 11.8 ms slower than response times during correct Go trials that followed a previous correct Go trial (940.0 ± 18.5 ms versus 800.9 ± 17.4 ms; $t(33) = 11.75$, $p < 0.001$, paired t -test). These differences were significant at the within session level in the majority of individual experimental sessions (26 of 34 experimental session, $p < 0.05$, unpaired t -test). Moreover, across sessions, participants committed more errors during Go trials following correct Conflict trials than during Go trials following previous correct Go trials ($6.7\% \pm 1.0$ versus $1.3\% \pm 0.4$; $t(33) = 5.23$, $p < 0.001$, paired t -test). Similar to the across-trial adjustments that occurred following the more difficult Conflict trials, response times were also significantly longer during correct Go trials that followed errors than during correct Go trials that followed correct trials (871.8 ± 24.6 ms versus 820.6 ± 17.0 ms; $t(33) = 2.66$, $p < 0.05$, paired t -test).

Within-Trial Conflict and Movement Signals

During the operative procedure, we simultaneously captured micro and macroelectrode recordings from the subthalamic nucleus (STN) and intracranial EEG (iEEG) from subdural electrodes temporarily placed over the medial prefrontal cortex (mPFC) as participants performed the task (Fig. 1c; Supplementary Fig. S1). We first investigated the overall changes in spectral power in both the STN and the mPFC during all correct trials compared to a baseline period (Fig. 1d,e). Overall theta band (2-5 Hz) activity increased following the presentation of each arrow (cue) in both the STN and mPFC (Supplementary Fig. S2). In both cases, the increases occurred prior to the response, however theta power peaked significantly earlier in the mPFC than in the STN (593 ± 76 ms versus 876 ± 86 ms; $t(61) = 2.46$, $p < 0.01$, unpaired t -test). Conversely, the changes over the broad 8-30 Hz range, which hereafter we will term beta activity for convenience, were different in the STN and the mPFC during the task. Overall beta power decreased prior to the response in the STN, but increased in the mPFC and peaked after the movements were made (Fig. 1d,e; Supplementary Fig. S2). In our analysis we distinguished neural signals dictated by each cue and its corresponding response (within-trial effects) from those conditioned by past cues and responses (across-trial effects).

Within each trial, we first examined how the output multiunit spiking activity (MUA) of the STN is modulated using the microelectrode recordings. The majority of recordings (39 out of 49) individually demonstrated significantly higher MUA during the task compared to baseline ($p < 0.05$, permutation test; see Materials and Methods). However, even within these recordings, spiking activity was heterogeneous (Fig. 2a; Supplementary Fig. S3). Some recordings demonstrated higher MUA during Conflict and NoGo trials, whereas others demonstrated higher MUA during trials with movement (Go and Conflict trials). Overall, when we examined differences in MUA activity across the three trial types in all recordings, we found that Conflict trials exhibited the highest level of MUA within each trial, followed by Go trials, and then NoGo trials ($p < 0.05$, permutation test; Fig. 2b). We confirmed these differences by examining neuronal spiking activity identified using voltage threshold detection (Supplementary Fig. S4).

We next examined how the within-trial changes in theta power observed in both the STN and mPFC between the cue and the response differ between the three trial types. The STN and the mPFC both demonstrated significantly higher pre-response theta power during the more difficult Conflict trials compared to the easier Go trials ($p < 0.05$, permutation test; Fig. 3a; Supplementary Fig. S5 and Supplementary Fig. S6; post-response differences between Go and Conflict trials are most likely an extension of the post-response beta band differences between trials types discussed below). The NoGo trials, however, during which no movements were made, showed the largest theta power increases in the mPFC and the smallest increases in the STN.

Because of the similar increases in theta power we observed in both brain regions during the task, we also investigated whether there were any changes in phase coherence between the mPFC and STN during the task. Across all trials, we found significantly greater theta band phase coherence during the task compared to the baseline period ($p < 0.05$, permutation test; Fig. 3c). When we compared the three trial types, we found significantly higher levels of theta phase coherence during Conflict and NoGo trials compared to Go trials ($p < 0.05$, permutation test; Fig. 3d). There were no significant changes in beta band phase coherence compared to baseline.

Within each trial, we also examined the changes in beta band power in the STN and found a significant decrease

within the first 500 ms following the cue during all three trial types (Fig. 4a). The decrease in beta power within each trial was accompanied by a significant decrease in coupling between STN beta oscillatory phase and MUA amplitude compared to the baseline period ($p < 0.05$, permutation test; Supplementary Fig. S7). Notably, the decrease in beta power was aborted earlier during NoGo trials, resulting in a significant difference in beta power between trials that involved movement (Go and Conflict) and those that did not (NoGo; $p < 0.05$, permutation test; Fig. 4a; Supplementary Fig. S5). This reversal in NoGo beta band activity began early enough to be involved in stopping any movement response, which otherwise occurred approximately 350 ms later. We found no significant differences in cue-aligned beta power between Go and Conflict trials ($p > 0.05$, permutation test; response aligned differences are due to the differences in relative timing of the cue when aligned to the response).

A prior study has suggested that premature decreases in beta power may be associated with the erroneous execution of prepotent actions (24). We therefore analyzed the relatively few errors that participants made in order to examine whether the decreases in STN beta power were altered during error trials (Fig. 5a; mean 10.8 ± 1.4 error trials per experimental session). We found a significantly lower level of STN beta power within the first 500 ms of error trials compared to either Go or Conflict trials ($p < 0.05$, permutation test; Fig. 5b; see Supplementary Fig. S8 for STN spiking data during errors). These differences were locked to the cue and could not be due to the differences in movement onset as there was no significant difference in response times between error trials and correct Go trials (811.7 ± 26.6 ms versus 831.5 ± 17.2 ms; $t(31) = 0.76$, $p > 0.05$, paired t -test).

Post-response adaptations in the mPFC

Increases in overall beta activity in the mPFC occurred following the movement response (Fig. 4e). We therefore examined the increases in beta band activity in the mPFC for all three trial types, and found significantly higher beta power in the mPFC during Go trials compared to Conflict trials ($p < 0.05$, permutation test; Fig. 4b; Supplementary Fig. S6). Importantly, these differences occurred after the participants executed the movement response. Furthermore, we found no significant differences between the Go and NoGo trials in the cue-aligned data, as both showed a very similar increase during the task. This suggests that the observed differences in mPFC beta activity between the Conflict trials and the Go and NoGo trials were strictly related to the difficulty of the completed trial, and not to movement.

The attenuated increases in mPFC beta power following Conflict trials suggest that beta oscillations may be involved in the recruitment of additional resources used for cognitive control following Conflict. Errors often recruit similar resources (38). We therefore analyzed the relatively few errors that participants made in order to examine whether the changes in mPFC beta activity were similar following error or Conflict trials (Fig. 5c). Unlike the increases in mPFC beta activity observed following correct trials, we found that error trials exhibited a significant decrease (relative to baseline) in mPFC beta activity following the response. The post response changes in beta power were significantly different between the error trials and the correct Go and correct Conflict trials ($p < 0.05$, permutation test; Fig. 5d). Moreover, error trials also demonstrated a significant increase in mPFC gamma power following the response ($p < 0.05$, permutation test; Fig. 5c; Supplementary Fig. S9).

Across-trial adaptations

We observed slower response times in correct Go trials that followed a previous correct Conflict trial (Fig. 1b). As such, we investigated whether beta activity in the mPFC or STN was different during Go trials that followed previous Conflict trials compared to Go trials that followed previous Go trials. We only included in this analysis trials during which participants responded correctly on both adjacent trials. Importantly, the stimuli presented in the subsequent Go trials in this analysis were identical, and the primary difference between the trial types of comparison here was what had occurred during the previous trial.

We found significantly higher levels of STN beta power during correct Go trials following correct Conflict trials compared to correct Go trials following previous correct Go trials ($p < 0.05$, permutation test; Fig. 6a). These higher levels of STN beta power occurred in the first 200 ms of the subsequent Go trial. This was a time period which did not show any significant differences when we compared the Go, NoGo, and Conflict trials (Fig. 4a), but did show significantly lower beta power during the error trials (Fig. 5b). In contrast, we found no significant differences in mPFC beta power during the execution phase of the second trial (Fig. 6b), suggesting that if mPFC beta activity is involved in across-trial adaptations to conflict, this involvement is only reflected in the time period immediately following the previously completed trial.

Because correct Go trials also showed slower response times when they followed an error trial, we also examined whether the commission of an error on the previous trial affected mPFC and STN beta power on subsequent correct Go trials. We only included in this analysis trials during which a participant incorrectly responded to the stimulus on the previous trial, but then correctly responded to stimulus on the subsequent Go trial. Like the response to previous Conflict, STN beta power during Go trials following errors was significantly higher than STN beta power during Go trials following correct trials ($p < 0.05$, permutation test; Fig. 6c). These differences were also locked to the Go cue and occurred within the first 200 ms of the subsequent Go trial. Also in line with the response to previous Conflict, we found no significant differences in mPFC beta power during the execution phase of the second trial (Fig. 6d), further suggesting the the mPFC's involvement in across-trial adaptations to errors is restricted to the time period immediately following the error. Analyzing STN theta power and MUA amplitude during across-trial adaptations to Conflict or error trials did not show any significant differences between trial types (data not shown).

Discussion

Our data demonstrate that the STN and the mPFC play complementary roles as individuals use cognitive control to monitor for conflicts and errors and to adjust subsequent actions accordingly. Theta oscillatory activity is coordinated between the mPFC and the STN when detecting conflict within an ongoing trial. Actions within that trial may then be facilitated by decreased beta activity only in the STN, and these decreases exhibit an early return to baseline when individuals inhibit a response. Following a trial, however, changes in beta activity in the mPFC, but not the STN, reflect the extent to which the completed trial was easy or difficult, or whether an error occurred. This information is then associated with an initial elevation of STN beta power in the subsequent trial, possibly contributing to the longer response times seen following conflict and error trials. The trial type related differences in theta and beta power are summarized in schematic form in Fig 7 (See Supplementary Fig. S5 and Supplementary Fig. S6 for spectrograms showing the trial type related differences for the STN and mPFC, respectively).

The novel response inhibition task used here requires movement while monitoring for conflict and for errors, processes that collectively support cognitive control (1, 2, 3). In several respects, the Go and NoGo trials are relatively easy, and require a simple translation from a cue on the screen directly to a movement (or withholding thereof). In contrast, Conflict trials are more difficult, as suggested by the slower reaction times and higher error rates. They require greater cognitive control in order to overcome a prepotent response in the direction of the arrow and move in the opposite direction. Once completed, these trials then elicit an appropriate adjustment for the next trial, which manifests itself as a slower response time.

Contrasting within-trial effects of theta oscillations in the mPFC and STN

Within a given trial, a participant must resolve the conflicts induced by the visual stimulus, decide whether and in what direction a movement must occur, and delay actions until that decision is made. Here, the mPFC and STN seem to coordinate their activity. Relative to Go trials, Conflict results in higher theta power in both the mPFC and the STN and higher theta phase coherence between the two brain regions. These results are consistent with previous studies demonstrating the role of theta communication between these regions during conflict (31, 32). Notably, the NoGo trials exhibit the highest levels of theta power in the mPFC as well as the highest theta phase synchrony between the mPFC and the STN. To our knowledge, no prior work has shown increased phase synchrony between these two brain regions when participants are instructed to completely withhold an action. These data therefore lend the strongest support yet to the hypothesis that mPFC-STN theta coherence conveys an anti-kinetic signal that can either cancel a movement entirely or slow down a response in the presence of conflict (4, 5, 39, 18).

Theta activity in the STN, however, diverges from that of the mPFC during the NoGo trials, as these trials evoke the smallest, rather than largest, increases in STN theta power. Intriguingly, multiunit spiking activity seems to follow a very similar pattern of trial type related differences. STN theta power and MUA are both lowest during the NoGo trials that involve no movement and peak at the time of the response during Go and Conflict trials, suggesting an involvement in the execution of the movement. Together, these data would appear inconsistent with classical

models of basal ganglia circuitry in which the STN is presumably involved in activating the inhibitory indirect pathway (19, 20). However, more recent evidence has suggested that indeed most STN neurons increase, rather than decrease, spiking activity during movement (40, 36, 41), and increased STN theta activity has been implicated in pathologies that involve excess movement such as dystonia, dyskinesia, and impulsivity (42, 43, 44, 45).

This, then, presents a paradox; why should elevated levels of mPFC theta power and mPFC-STN phase synchrony be anti-kinetic while STN theta power facilitate movement? One possibility may be that the differences in theta oscillatory activity are related to the specific neural circuits in which they are expressed. The increases in mPFC theta power and in mPFC-STN phase synchronization occur early and are separable in time from the increases in STN theta activity both in our current paradigm and in prior studies (31, 32, 46). Thus, the relative timing of increases in theta power may be consistent with the sequential engagement of two circuits converging on the STN, one conveying information regarding conflict early in a trial and a second that is responsible for a more explicit motor drive. Another possibility, however, is that both theta and spiking activity are indeed inhibitory in nature as originally proposed in the classical models (19, 20). Early in the trial, they may globally inhibit all movements while the appropriate action is being selected. During the response, however, they utilize a center-surround architecture (40) to selectively inhibit only undesired movements that would otherwise interfere with the correct action. In this scenario, NoGo trials demonstrate an abrupt termination of theta power and MUA because no movements are executed, making any inhibition of irrelevant movements unnecessary. Our data cannot distinguish these possibilities, and the precise role of theta activity in the STN still remains unresolved.

Contrasting within-trial and across-trial adaptation effects of beta oscillations in the mPFC and STN

The contrasting roles of beta activity in the STN and the mPFC during this task provide an even clearer exposition of the principle that the behavioral associations of oscillatory activity reflect the complementary roles of these structures. Not surprisingly, beta activity in the STN was directly related to movement itself, decreasing following the Go and Conflict cues and remaining attenuated until the response. These decreases prematurely return to resting levels during NoGo trials that require complete response inhibition, consistent with previous studies investigating STN beta activity when motor and non-motor actions are stopped (21, 22, 25, 26, 27, 41). Of note, the reductions in STN beta band power during each movement trial were accompanied by a significant reduction in beta band spiking entrainment. Given that movement also results in an overall increase in spiking activity, these changes suggest that beta may serve as a gate for action in the STN. Resting levels of beta power and spike entrainment may impede processing related to movement, while reduced levels free the STN neurons to encode a diverse variety of task relevant spiking patterns, as we observe in our data (Supplementary Fig. S3). Previous empirical and theoretical observations in the basal ganglia support this interpretation (47, 48, 49).

The trials that follow conflicts or errors further support the hypothesis that beta activity in the STN is antikinetic in nature. Both Conflict and error trials evoke longer response times in the subsequent trial, as individuals have adjusted their behavior to the unexpected outcome on the previous trial. Importantly, in the STN, beta band power is significantly elevated at the beginning of these subsequent trials. To our knowledge, this is the first study to

provide clear evidence that beta band activity in the STN increases in response to higher levels of cognitive control required by a previous trial, and that these increases are associated with slower response times. This is consistent with the suggestion that elevated beta band STN activity suppresses automatic pre-potent responses in favor of more goal oriented behavior (33). This framework also provides insight into our observation that trials with errors of commission exhibit significant early decreases in beta band activity. These decreases could cause the inappropriate early release of more automatic pre-potent responses. In the context of drift diffusion models, this would reflect a decreased decision threshold that would predispose an individual to automatic, non-goal oriented actions and lead to premature erroneous responses (28).

Beta band activity in the mPFC, on the other hand, changes very little within each trial but increases immediately following the response. Importantly, unlike the STN, the increases in mPFC beta activity following each trial are related to the difficulty of the trial itself, and not to whether a movement occurs. These increases were significantly attenuated following Conflict trials, and even reversed following errors. Few studies have analyzed mPFC activity during a Go-NoGo task (50), and most studies of mPFC oscillatory activity during response inhibition have focused on surface EEG changes in the theta band (3). Nevertheless, several lines of evidence suggest that decreased levels of mPFC beta activity after Conflict and error trials may be related to across-trial cognitive control. First, in our data, these changes in mPFC beta activity only occur following the completion of the trial, and any differences in mPFC beta activity are related to difficulty rather than movement. Moreover, as in our data, conflicts and errors are thought to recruit similar mPFC resources when higher levels of cognitive control are needed to adjust behavior or to prevent subsequent errors (38, 7, 8, 51, 6). Finally, errors necessarily imply some uncertainty regarding what the predicted outcome of an action was, or will be. Recent evidence has demonstrated that both internally generated and externally induced errors during sensorimotor adaptation tasks result in attenuations of the post-response increases in mPFC beta power, thereby linking these changes in mPFC beta power to this aspect of cognitive control (52).

Beta oscillations and predictive coding during cognitive control

Indeed, the observed changes in mPFC and STN beta activity may in fact be consistent with models of predictive coding as they relate to the various cognitive and motor aspects of this task (53). This task generally requires following a simple rule, to move in the direction of an arrow. On occasion however, and therefore unexpectedly, there is a change in the rule, and participants must move in the opposite direction. During these instances, there is both sensorimotor conflict regarding which way to move, and a prediction error related to which rule the participant was expecting to follow. Increasing evidence suggests that cortical processing is optimized for predictive coding, and that such top-down predictions are conveyed through beta oscillatory activity (54, 55, 56, 57). The neural mechanisms for predicting a set of task rules should be analogous, and in this case would involve areas like the mPFC that have been implicated in setting goals and rules (1, 2, 3). The reductions in mPFC power following Conflict or errors would, according to this paradigm, reflect a switch from a top-down state in which predictions are weighed more heavily to a bottom-up state in which there is greater uncertainty regarding previously held expectations (54, 55). The observed increases in high gamma activity following both Conflict and error trials support this possibility as

gamma oscillations have been linked to bottom-up sensory driven processes (56, 57).

A similar framework linking beta activity to predictive coding may also be relevant for interpreting the changes observed in STN beta activity with movement (53). Although such a link between STN beta activity and prediction has yet to be firmly established, these models posit that beta oscillations reflect predictions related to the expected state of sensory inputs and how those inputs may or may not change with movement. When making a movement, one must actively discard predictions related to the current sensory state, as those inputs will surely change with movement. This results in a decrease in beta activity. Conversely, if beta remains elevated, it is difficult to make a movement because it is difficult to change those predictions and anticipate a new sensory state. In these cases, higher beta activity maintains the status quo (58, 59, 53). Hence, it is possible that the observed changes in beta activity in both the mPFC and the STN are related to the extent to which predictions regarding the task are met or violated, and that the distinction between the two structures reflects the distinction in the types of predictions that are relevant. On the one hand, STN beta signals are strictly related to the action, whereas mPFC beta signals are related to the expectations regarding the task rules.

Taken together, our results evidence the broad principle that oscillatory neuronal activity at the same frequency in different circuits may be associated with different behavioral effects (60). This is achieved by the coordinated sequencing of these neural activities. Specifically, we have provided evidence that although beta activity may be considered anti-kinetic when expressed in the STN prior to movement, in the mPFC it is associated with the modulation of cognitive control necessary following response evaluation. Similarly, although early increases in mPFC and STN theta power and phase synchrony may be considered anti-kinetic, later theta power increases in the STN may actually promote movement. Our inferences are drawn from data collected in patients with Parkinson’s disease, and so should be interpreted with caution as dopamine depletion and DBS surgery are known to alter the activity of the basal ganglia (61). Nonetheless, we find that patterns of theta and beta band activity in the STN and mPFC play complementary, temporally sequenced roles in supporting different processes that together contribute to cognitive control.

Materials and Methods

Intraoperative task and recordings during deep brain stimulation surgery

We made intraoperative recordings in 22 participants undergoing deep brain stimulation (DBS) surgery of the subthalamic nucleus (STN) for Parkinson’s disease. The study was conducted in accordance with an NIH IRB approved protocol, and all participants gave their written informed consent to take part in the study. Participants received no financial compensation for their participation. Parkinson’s disease medications were stopped on the night before surgery (12 h preoperatively). We recorded while participants were alert, at rest and supine, and in an OFF state in the operating room. Sample-size estimation computations were not conducted prior to data collection. Instead, during a two year period (April 2014-April 2016) data were collected during all DBS cases in which the patient was willing and able to participate in the task. The goal was to collect between 10-20 recording sessions during this 24 month time period. Approximately one DBS case was done per month resulting in 22 total cases. The raw electrophysiology data and relevant code will be made available here: <https://neuroscience.nih.gov/ninds/zaghloul/downloads.html>

As per routine DBS surgery, we used intraoperative microelectrode recordings to identify the STN based on firing rate and pattern (increased spiking activity and background noise relative to the more dorsal zona incerta and thalamus). We simultaneously advanced three targeting electrodes, separately spaced 2 mm apart, during each recording session (placed along a central, 2mm lateral, and 2mm anterior trajectory; Fig. 1c). Each targeting electrode consisted of a microelectrode contact and a macroelectrode contact positioned 3 mm dorsal to the microelectrode tip (Alpha Omega, Alpharetta, GA). Macroelectrode contacts were within the STN if the corresponding microelectrode contact was greater than 3 mm ventral to the dorsal border of the STN (identified by increased spiking activity and background noise relative to the more dorsal zona incerta and thalamus). We restricted all analyses only to signals captured from electrode contacts positioned within the STN. Raw signals were sampled at 1.5024 and 24.0345 kHz from macro and microelectrode contacts, respectively, and stored using a MicroGuide Pro data acquisition system (Alpha Omega Co., Alpharetta, GA).

During the operative procedure, we acquired simultaneous intracranial EEG (iEEG) recordings from a subdural strip electrode temporarily placed through the DBS burrhole (PMT Corporation, Chanhassen, MN). We placed a six-contact mPFC strip electrode consisting of a single row of six platinum contacts (2.3 mm exposed diameter with 1 cm inter-contact spacing) in a direct anterior direction from the burr hole. The electrodes were placed on the medial superior portion of the prefrontal cortex, and thus we will refer to the area from which we recorded as the medial prefrontal cortex (mPFC). We confirmed contact localization using intraoperative x-ray (Supplementary Fig. S1). In 20 of the 34 sessions, we also placed an eight-contact lateral PFC strip electrode in a direction that was angled approximately 60 degrees lateral to the direction of the mPFC strip electrodes as a part of a separate study. In two of the experimental sessions, we did not implant any iEEG strip electrodes. All subdural strip electrodes were removed after completion of the behavioral task on each side.

Behavioral task

Participants performed a novel response inhibition task (Fig. 1a) in the intra-operative environment on a testing laptop running Psychopy (62). The task involved one continuous block of 200 trials. On each trial, a white fixation dot initially appeared in the center of the screen for 500 ms. We subsequently displayed an arrow in the center of the screen pointing in either the leftward or rightward direction. The color of the arrow could be either blue or red. If the arrow was blue (Go trials), then the participant was required to move a digital joystick in the direction the arrow was pointing. If the arrow was red (Conflict trials), then the participant was required to move the joystick in the opposite direction of the arrow. If, however, the arrow had a white border around it (NoGo trials), the participant was instructed to withhold all movements until the arrow disappeared from the screen. Out of the 200 trials in each session, 120 were blue arrow Go trials, 40 were red arrow Conflict trials, and 40 were white border NoGo trials. The color of the arrow on the NoGo trials was blue on 30 of the trials and red on 10 of the trials (consistent with the overall 3:1 ratio of blue:red arrows), although this information was irrelevant given that the subjects were withholding a response on these trials.

Participants made all movements with the hand contralateral to the side of intra-operative recording for that session. All participants who completed the task were sufficiently able to control the joystick. Patients with a tremor that was severe enough to interfere with control of the joystick were unable to perform the task and therefore excluded from the study. 150 ms following each response, subjects were given feedback for that trial. If the participant correctly moved the joystick in the appropriate direction for the Go or Conflict trials or if the subject correctly withheld a response in the NoGo trials, we presented a green smiley face and the word "CORRECT" in the center of the screen. If the subject moved the joystick in the incorrect direction for the Go and Conflict trials or moved the joystick in any direction for the NoGo trials, we presented a red sad face and the word "WRONG." We subsequently refer to these trials with an incorrect response as 'error' trials. The duration of the feedback stimulus was 500 ms. Following the feedback, we displayed a blank screen for a duration randomized between 1000 ± 100 ms, before presenting the warning cue for the subsequent trial.

Three strategies were employed to encourage the subjects to respond in a timely manner. First, the subjects were encouraged ahead of time to respond quickly while trying to minimize errors. Second, if the subjects took longer than 1500 ms to respond, their response was not recorded and the feedback they received consisted of a yellow neutral face and the phrase, "Please respond faster". Third, the arrows were only displayed on the screen for 1000 ms. We discarded all trials with response times less than 300 ms and greater than 1500 ms.

On the day before surgery, participants performed a complete session in order to familiarize themselves with the task. During the operative procedure, most participants performed one session while we captured recordings from the left STN and a second session while we recorded from the right STN. Ten participants did not complete the second session because of fatigue. This resulted in 34 total intra-operative recording sessions included in the analysis. Most of the analyses we conducted included only correct trials. Accordingly, when we analyzed any across-trial changes in behavior and electrophysiology, only trials in which the current trial and the previous trial were both correct were included in the analysis. When we specifically analyzed the error related changes in electrophysiology, we only

included the 27 sessions in which subjects committed 5 or more errors. When we specifically analyzed the post-error related changes that occurred on the correct Go trials that followed an error trial, we only included the 19 sessions in which subjects committed 5 or more errors and had 5 or more correct Go trials that followed an error trial.

LFP and iEEG power

We performed all analyses using MATLAB (Mathworks, Natick, MA). We extracted local field potential (LFP) activity from each macroelectrode and iEEG activity from each subdural contact. We bandpass filtered both signals between 1 and 500 Hz, notch filtering at 60 Hz, and downsampled the data to 1 kHz. We referenced the macroelectrode and iEEG signals by subtracting the signals of adjacent electrodes. For each session, this generated three referenced bipolar LFP channels for the STN and five referenced bipolar signals for the mPFC strip. We henceforth refer to these bipolar channels as electrode contacts. Prior to any subsequent analysis, we discarded all trials exhibiting a clear artifact in the LFP or iEEG trace.

In order to obtain magnitude and instantaneous phase information in the frequency domain, we convolved the LFP signals captured from the STN and iEEG signals captured from the subdural contacts from each trial with complex valued Morlet wavelets (wave number 6). We used 47 logarithmically spaced (8 scales/octave) wavelets between 2 and 107 Hz and convolved each wavelet with 3000 ms of LFP data from each trial. For cue-locked analyses, we analyzed LFP signals from 1000 ms before to 2000 ms following arrow presentation. For response-locked analyses, we analyzed LFP signals from 1500 ms before to 1500 ms after the response. We used a 1000 ms buffer on both sides of the clipped data to eliminate edge effects. We squared the magnitude of the continuous-time wavelet transform to generate a continuous measure of instantaneous power for each frequency. We determined the z-scored power from each channel and frequency using the mean and standard deviation of the power recorded from that channel during a baseline period. We defined the baseline period as the 500 ms preceding the presentation of the fixation cue. Though several of our findings show significant differences during the time period in between adjacent trials, none of these differences extended into this baseline period.

For each STN recording, we averaged the normalized power from macroelectrodes that were within the STN as identified during the operative procedure. Because we did not have access to intraoperative computed tomography (CT) imaging, we were unable to use patient specific landmarks to accurately localize individual iEEG contacts. Thus, for each iEEG strip, we averaged the normalized power from all five bipolar channels recorded from that strip. This procedure resulted in one spectrogram for the STN and one for the mPFC during each trial.

Statistical analysis

To assess differences in spectral power between conditions across recording sessions, we first calculated the trial-averaged normalized power for all three conditions in each region in each experimental session. In order to prevent the 3:1:1 ratio of Go:Conflict:NoGo trials from affecting our results, we subsampled the correct Go trials prior to taking the average. Subsampling was achieved by randomly selecting a subset of the correct Go trials to match the number of correct Conflict trials and then calculating the average across only that subset of correct Go trials.

Due to the difference in error rates between the Conflict and the NoGo trials, we also subsampled the correct NoGo trials to match the number of correct Conflict trials. We were therefore left with an average normalized power for Go, Conflict, and NoGo trials of similar trial number at each time point and frequency for each session. We also used subsampling when comparing the error trials to correct trials or when comparing the Go trials that followed a previous Go trial to the Go trials that followed a Conflict trial. To test for any trial type related differences in power, we performed random-effects statistical analyses in each region across sessions. For each comparison, our null hypothesis was that across sessions, there was no difference in normalized power between trial types (Go versus Conflict, NoGo versus Go, NoGo versus Conflict, etc). In order to assess overall changes in power during the task regardless of condition, we used a similar statistical analysis. In this case, our null hypothesis was that the average power across all trials was not different from zero. We tested these hypotheses using a non-parametric permutation procedure in which the session is the unit of observation (63).

In each region, we computed the true mean difference across sessions between the two conditions being compared (Go versus Conflict, NoGo versus Go, NoGo versus Conflict, all trials versus baseline, etc) for every time point and frequency. We then randomly permuted the condition specific averages for each session and recomputed the mean difference across sessions. We repeated the permutation 200 times to generate an empirical distribution of possible mean differences that were all equally probable under the null hypothesis. For every time-frequency point, we compared the true mean difference to the mean and standard deviation of the corresponding point in the empirical distribution to generate a p-value. This p-value represents the likelihood that the true mean difference for each time-frequency point represents a departure from the null hypothesis. However, this p-value for each time-frequency point does not take into account the multiple comparisons that are made across all time points and frequencies.

To correct for multiple comparisons across all time points and frequencies, we used a cluster correction method based on exceedance mass testing (63). This method assumes that a true effect at any time-frequency point is likely to be observed across multiple time points and frequencies. We defined time-frequency clusters by thresholding the across-session p-values derived from the statistical analysis described above. Any contiguous time-frequency points with a p-value less than 0.05 were included in each cluster. For each identified cluster, we defined a cluster statistic to be the sum of the z-scores, derived from the p-value using a normal cumulative distribution function, for all time-frequency points within that cluster.

We calculated clusters using the true data, and for each of the 200 permutations of the session-specific trial averages. We used the maximum cluster statistic of each permutation to create an empirical distribution for significance testing. We determined whether a true cluster test statistic was significant by comparing it to the empirical distribution of maximum cluster test statistics. In this manner, significant clusters can arise from large differences between trial types that extend over a small number of frequencies or over a small time period, or from smaller differences that involve a larger number of time-frequency points. We considered cluster test statistics with $p < 0.05$ to be significant and corrected for multiple comparisons.

We also tested for significant differences in power within two specific frequency bands of interest (2 - 5 Hz and 8-30 Hz) based on the overall changes in power observed during the task relative to the baseline period. We used

the same permutation procedure described above, but first averaged spectral power across the frequency band of interest prior to calculating any true or surrogate differences between conditions. In this case, clusters were based on contiguous time points exhibiting significant differences across sessions.

STN-cortical phase coherence

To estimate the time-varying inter-site phase coherence, between the STN and the mPFC, we used the continuous time wavelet transform data extracted above for each trial and each frequency (see 'LFP and iEEG Power'). We first calculated the difference at each time-frequency point between the instantaneous phase (projected on the complex plane) in the LFP signal and the instantaneous phase in the iEEG signal. To generate a continuous-time estimate of phase coherence, we calculated the magnitude of the average difference over 250 ms sliding windows (step size 1 ms) (64). This results in a time-varying estimate of phase coherence for every frequency, for every trial, and for every pair of electrodes.

We determined the z-scored phase coherence for each pair of electrodes at each time-frequency point by comparing the continuous measure of phase coherence to the mean and standard deviation of the phase coherence recorded from that pair of electrodes during the baseline period. As with the analysis of power, we subsampled the Go and NoGo trials to match the number of correct Conflict trials and then averaged the z-scored phase coherence across trials. We averaged the z-scored phase coherence across all contacts within the iEEG strip and then averaged across all macroelectrodes that were within the STN as identified during the operative procedure. We therefore generated a single average phase coherence spectrogram between the mPFC and the STN for each condition for every session. In order to compare differences in phase coherence between conditions across all sessions, we used the same across-session permutation procedure described above.

Spiking activity

We extracted spiking activity by bandpass filtering microelectrode recordings between 0.3 and 3 kHz and resampling the filtered signals at 24 kHz. For the purposes of plotting spiking activity raster plots and generating a time series of spiking activity (Fig. 2), we identified spike events by manually setting a negative or positive voltage threshold depending on the direction of the voltage deflection (Plexon Offline Sorter, Inc., Dallas, TX). Given the difficulty of isolating single unit activity in the STN (65, 66), we used the technique outlined by Stark and Abeles (67) to identify STN multiunit activity (MUA). We measured the MUA by clipping extreme values in the band passed filtered data (larger or smaller than the mean 2 STDs) and computing the root mean squared (RMS). We computed the RMS by squaring the data, low pass filtering at 100 Hz, downsampling to 1000 Hz, and taking the square root. Finally, we smoothed the resulting MUA data using a Gaussian kernel (standard deviation 50 ms). Though most of our analysis of STN spiking involved the MUA data, repeating the analysis using the more traditional voltage threshold method produced very similar patterns of activity for task responsive recordings (see Supplementary Fig. S3 and Supplementary Fig.S4). For this confirmatory analysis, we calculated the continuous-time firing rates for each recording by smoothing the spike train (generated by manual thresholding, see above) from each trial (1 ms bins)

with a Gaussian kernel (standard deviation 50 ms). The MUA analysis was chosen over this method as it seemed less prone to noise in the recording and did not depend on a manually chosen arbitrary threshold being applied to all time periods of the recording. It is important to note, however, that MUA activity is thought to reflect a composite of the highly focal firing rate of neurons, bursting, recruitment, and synchronization effects (68).

We extracted 3000 ms of MUA data from each trial for each microelectrode. We excluded all trials with an MUA greater or less than 15 standard deviations from the average MUA across all trials. To generate a normalized average MUA, we compared MUA for each trial to the mean and standard deviation of the MUA firing during the baseline period and then averaged across trials. To determine whether an individual microelectrode recording exhibited a significant change in MUA during the task, our null hypothesis was that the average MUA across all correct trials (Go, Conflict, NoGo) was not different than zero. For each recording, we used the same permutation procedure described above to compare the true mean continuous MUA across all trials to an equally sized trial- by-time matrix of zeros. For these within-subject comparisons, however, the unit of observation being permuted was the individual trial. Any MUA recording with a contiguous cluster of p-values < 0.05 was considered responsive.

From the 34 STNs we included in our analyses, we identified 49 MUA recordings (from 22 different STNs) that were within the borders of the STN. 39 (79.6%) of the recordings (from 20 different STNs) showed an increase in MUA firing during the task. Out of the 10 recordings that did not show a significant increase in MUA during the task, 5 showed a significant decrease, and 5 showed no changes. Nevertheless, for the across-session analysis of trial-type related MUA changes all 49 recordings were included. Rather than treat each of these 49 recordings as independent, however, we chose to combine recordings that were acquired from the same STN. Had we not done so, we would run the risk of artificially increasing the number of MUA recordings included in our statistical analysis as MUAs recorded from the same STN were more than likely not independent. Indeed, we found that there was often a similar pattern of task related MUA changes in different electrodes recorded from the same STN. To address this issue, we average the normalized MUA of responsive electrodes recorded from the same STN. Thus, each of the 22 STN recording sessions with spiking activity resulted in just one measurement of MUA activity that we subsequently used in our across-session analyses when comparing trial types.

To determine if the STN MUAs exhibited a significant difference between trial types (Go versus Conflict, NoGo versus Go, NoGo versus Conflict, etc) across sessions, for every STN we calculated the mean difference in firing at every time point between trial types. We then calculated the average difference across all 22 STNs and compared the difference to an empirical distribution generated by permuting the condition labels of each session’s average data 200 times. We corrected for multiple comparisons across time using the same nonparametric clustering-based procedure described above.

References

- [1] Miller, E. K. & Cohen, J. D. An Integrative Theory of Prefrontal Cortex Function. *Annual Review of Neuroscience* **24**, 167–202 (2001).
- [2] Ridderinkhof, K. R., Ullsperger, M., Crone, E. A. & Nieuwenhuis, S. The Role of the Medial Frontal Cortex in Cognitive Control. *Science* **306**, 443–447 (2004).
- [3] Cohen, M. X. A neural microcircuit for cognitive conflict detection and signaling. *Trends in Neurosciences* **37**, 480–490 (2014).
- [4] Cavanagh, F., James *et al.* Subthalamic nucleus stimulation reverses mediofrontal influence over decision threshold. *Nat. Neurosci.* **14**, 1462–1467 (2011).
- [5] Cohen, M. X. & Cavanagh, J. F. Single-trial regression elucidates the role of prefrontal theta oscillations in response conflict. *Front. Psychol.* **2**, 30 (2011).
- [6] Cavanagh, J. F., Zambrano-Vazquez, L. & Allen, J. J. B. Theta lingua franca: A common mid-frontal substrate for action monitoring processes. *Psychophysiology* **49**, 220–238 (2012).
- [7] Kerns, J. G. *et al.* Anterior Cingulate Conflict Monitoring and Adjustments in Control. *Science* **303**, 1023–1026 (2004).
- [8] Cavanagh, J. F., Cohen, M. X. & Allen, J. J. Prelude to and resolution of an error: Eeg phase synchrony reveals cognitive control dynamics during action monitoring. *J. Neurosci.* **29**, 98–105 (2009).
- [9] Cohen, M. X. & van Gaal, S. Subthreshold muscle twitches dissociate oscillatory neural signatures of conflicts from errors. *NeuroImage* **86** (2014).
- [10] Sheth, S. A. *et al.* Human dorsal anterior cingulate cortex neurons mediate ongoing behavioural adaptation. *Nature* **488**, 218–221 (2012).
- [11] Danielmeier, C., Eichele, T., Forstmann, B. U., Tittgemeyer, M. & Ullsperger, M. Posterior Medial Frontal Cortex Activity Predicts Post-Error Adaptations in Task-Related Visual and Motor Areas. *J. Neurosci.* **31**, 1780–1789 (2011).
- [12] Chinn, L. K., Pauker, C. S. & Golob, E. J. Cognitive control and midline theta adjust across multiple timescales. *Neuropsychologia* (2018).
- [13] Modirrousta, M. & Fellows, L. K. Dorsal medial prefrontal cortex plays a necessary role in rapid error prediction in humans. *J Neurosci* **28**, 14000–14005 (2008).
- [14] Narayanan, N. S., Cavanagh, J. F., Frank, M. J. & Laubach, M. Common medial frontal mechanisms of adaptive control in humans and rodents. *Nat Neurosci* **16**, 1888–1895 (2013).

- [15] Zavala, B., Zaghoul, K. & Brown, P. The subthalamic nucleus, oscillations, and conflict. *Mov Disord* **30**, 328–338 (2015).
- [16] Alexander, G. E., DeLong, M. R. & Strick, P. L. Parallel Organization of Functionally Segregated Circuits Linking Basal Ganglia and Cortex. *Ann. Rev. of Neurosci.* **9**, 357–381 (1986).
- [17] Aron, A. R., Behrens, T. E., Smith, S., Frank, M. J. & Poldrack, R. A. Triangulating a cognitive control network using diffusion-weighted magnetic resonance imaging (MRI) and functional MRI. *J. Neurosci.* **27**, 3743–3752 (2007).
- [18] Kelley, R. *et al.* A human prefrontal-subthalamic circuit for cognitive control. *Brain* **141**, 205–216 (2018).
- [19] Albin, R., Young, A. & Penney, J. The functional anatomy of basal ganglia disorders. *Trends Neurosci.* **12**, 10 (1989).
- [20] DeLong, M. Primate models of movement disorders of the basal ganglia. *Trends Neurosci.* **13**, 281–285 (1990).
- [21] Kuhn, A. *et al.* Event-related beta desynchronization in human subthalamic nucleus correlates with motor performance. *Brain* **127**, 735 (2004).
- [22] Ray, N. J. *et al.* The role of the subthalamic nucleus in response inhibition: Evidence from local field potential recordings in the human subthalamic nucleus. *NeuroImage* **60**, 271–278 (2012).
- [23] Leventhal, D. *et al.* Basal ganglia beta oscillations accompany cue utilization. *Neuron* **73**, 523–536 (2012).
- [24] Brittain, J.-S. *et al.* A role for the subthalamic nucleus in response inhibition during conflict. *J. Neurosci.* **32**, 13396–13401 (2012).
- [25] Alegre, M. *et al.* The subthalamic nucleus is involved in successful inhibition in the stop-signal task: A local field potential study in parkinson’s disease. *Exp. Neurol.* **239**, 1–12 (2013).
- [26] Benis, D. *et al.* Subthalamic nucleus activity dissociates proactive and reactive inhibition in patients with parkinson’s disease. *NeuroImage* **91**, 273–281 (2014).
- [27] Bastin, J. *et al.* Inhibitory control and error monitoring by human subthalamic neurons. *Transl Psychiatry* **4**, e439 (2014).
- [28] Herz, D. M. *et al.* Distinct mechanisms mediate speed-accuracy adjustments in cortico-subthalamic networks. *eLife* **6**, e21481 (2017).
- [29] Zavala, B. A., Jang, A. I. & Zaghoul, K. A. Human subthalamic nucleus activity during non-motor decision making. *Elife* **6** (2017).
- [30] Zaghoul, K. A. *et al.* Neuronal activity in the human Subthalamic Nucleus encodes decision conflict during action selection. *J. Neurosci.* **32**, 2453–2460 (2012).

- [31] Zavala, B. A. *et al.* Midline frontal cortex low-frequency activity drives subthalamic nucleus oscillations during conflict. *J. Neurosci.* **34**, 7322–7333 (2014).
- [32] Zavala, B. *et al.* Human subthalamic nucleus/medial frontal cortex theta phase coherence is involved in conflict and error related cortical monitoring. *NeuroImage* **137**, 178–187 (2016).
- [33] Frank, M. J., Samanta, J., Moustafa, A. A. & Sherman, S. J. Hold your horses: Impulsivity, deep brain stimulation, and medication in parkinsonism. *Science* **318**, 1309–1312 (2007).
- [34] Rushworth, M. F. S., Walton, M. E., Kennerley, S. W. & Bannerman, D. M. Action sets and decisions in the medial frontal cortex. *Trends Cogn. Sci. (Regul. Ed.)* **8**, 410–417 (2004).
- [35] Schuck, N. W. *et al.* Medial prefrontal cortex predicts internally driven strategy shifts. *Neuron* **86**, 331–340 (2015).
- [36] Goldberg, J. H., Farries, M. A. & Fee, M. S. Basal ganglia output to the thalamus: still a paradox. *Trends in Neurosciences* **36**, 695–705 (2013).
- [37] Jenkinson, N. & Brown, P. New insights into the relationship between dopamine, beta oscillations and motor function. *Trends in Neurosciences* **34**, 611–618 (2011).
- [38] Yeung, N., Botvinick, M. M. & Cohen, J. D. The Neural Basis of Error Detection: Conflict Monitoring and the Error-Related Negativity. *Psychological Review* **111**, 931–959 (2004).
- [39] Rae, C. L., Hughes, L. E., Anderson, M. C. & Rowe, J. B. The Prefrontal Cortex Achieves Inhibitory Control by Facilitating Subcortical Motor Pathway Connectivity. *J. Neurosci.* **35**, 786–794 (2015).
- [40] Nambu, A., Tokuno, H. & Takada, M. Functional significance of the cortico-subthalamo-pallidal ‘hyperdirect’ pathway. *Neurosci. Res.* **43**, 111–117 (2002).
- [41] Zavala, B. *et al.* Human Subthalamic Nucleus Theta and Beta Oscillations Entrain Neuronal Firing During Sensorimotor Conflict. *Cereb Cortex* **27**, 496–508 (2017).
- [42] Alonso-Frech, F. *et al.* Slow oscillatory activity and levodopa-induced dyskinesias in Parkinson’s disease. *Brain* **129**, 1748–1757 (2006).
- [43] Rodriguez-Oroz, M. *et al.* Involvement of the subthalamic nucleus in impulse control disorders associated with parkinsons disease. *Brain* **134**, 36–49 (2011).
- [44] Neumann, W.-J. *et al.* Enhanced low-frequency oscillatory activity of the subthalamic nucleus in a patient with dystonia. *Mov. Disord.* **27**, 1063–1066 (2012).
- [45] Neumann, W.-J. *et al.* A localized pallidal physiomaer in cervical dystonia. *Ann Neurol.* **82**, 912–924 (2017).

- [46] Pearson, J. M., Hickey, P. T., Lad, S. P., Platt, M. L. & Turner, D. A. Local Fields in Human Subthalamic Nucleus Track the Lead-up to Impulsive Choices. *Front. Neurosci.* **11** (2017).
- [47] Courtemanche, R., Fujii, N. & Graybiel, A. Synchronous, focally modulated beta-band oscillations characterize local field potential activity in the striatum of awake behaving monkeys. *J Neurosci* **23**, 11741–11752 (2003).
- [48] Mallet, N. *et al.* Disrupted Dopamine Transmission and the Emergence of Exaggerated Beta Oscillations in Subthalamic Nucleus and Cerebral Cortex. *J. Neurosci.* **28**, 4795–4806 (2008).
- [49] Brittain, J.-S. & Brown, P. Oscillations and the basal ganglia: Motor control and beyond. *Neuroimage* **85**, 637–647 (2014).
- [50] Yamanaka, K. & Yamamoto, Y. Single-trial EEG Power and Phase Dynamics Associated with Voluntary Response Inhibition. *Journal of Cognitive Neuroscience* **22**, 714–727 (2009).
- [51] Compton, R. J., Arnstein, D., Freedman, G., Dainer-Best, J. & Liss, A. Cognitive control in the intertrial interval: Evidence from EEG alpha power. *Psychophysiology* **48**, 583–590 (2011).
- [52] Tan, H., Wade, C. & Brown, P. Post-Movement Beta Activity in Sensorimotor Cortex Indexes Confidence in the Estimations from Internal Models. *J. Neurosci.* **36**, 1516–1528 (2016).
- [53] Friston, K. J., Bastos, A. M., Pinotsis, D. & Litvak, V. LFP and oscillations what do they tell us? *Current Opinion in Neurobiology* **31**, 1–6 (2015).
- [54] van Ede, F., Lange, F. d., Jensen, O. & Maris, E. Orienting Attention to an Upcoming Tactile Event Involves a Spatially and Temporally Specific Modulation of Sensorimotor Alpha- and Beta-Band Oscillations. *J. Neurosci.* **31**, 2016–2024 (2011).
- [55] Brown, H., Adams, R. A., Parees, I., Edwards, M. & Friston, K. Active inference, sensory attenuation and illusions. *Cogn Process* **14**, 411–427 (2013).
- [56] Engel, A. K., Fries, P. & Singer, W. Dynamic predictions: Oscillations and synchrony in topdown processing. *Nature Reviews Neuroscience* **2**, 704 (2001).
- [57] Buschman, T. J. & Miller, E. K. Top-Down Versus Bottom-Up Control of Attention in the Prefrontal and Posterior Parietal Cortices. *Science* **315**, 1860–1862 (2007).
- [58] Gilbertson, T. *et al.* Existing Motor State Is Favored at the Expense of New Movement during 13-35 Hz Oscillatory Synchrony in the Human Corticospinal System. *J. Neurosci.* **25**, 7771–7779 (2005).
- [59] Engel, A. K. & Fries, P. Beta-band oscillation signalling the status quo? *Current Opinion in Neurobiology* **20**, 156–165 (2010).
- [60] Fries, P. Rhythms For Cognition: Communication Through Coherence. *Neuron* **88**, 220–235 (2015).

- [61] Hammond, C., Bergman, H. & Brown, P. Pathological synchronization in parkinson’s disease: networks, models and treatments. *Trends Neurosci* **30**, 357–364 (2007).
- [62] Peirce, J. W. PsychoPyPsychophysics software in Python. *Journal of Neuroscience Methods* **162**, 8–13 (2007).
- [63] Maris, E. & Oostenveld, R. Nonparametric statistical testing of EEG- and MEG-data. *J. Neurosci. Meth.* **164**, 177–190 (2007).
- [64] Lachaux, J.-P. *et al.* Estimating the time-course of coherence between single-trial brain signals: an introduction to wavelet coherence. *Neurophysiologie Clinique/Clinical Neurophysiology* **32**, 157–174 (2002).
- [65] Weinberger, M. *et al.* Beta oscillatory activity in the subthalamic nucleus and its relation to dopaminergic response in parkinsons disease. *J Neurophysiol* **96**, 3248–3256 (2006).
- [66] Sharott, A. *et al.* Activity parameters of subthalamic nucleus neurons selectively predict motor symptom severity in parkinson’s disease. *J Neurosci* **34**, 6273–6285 (2014).
- [67] Stark, E. & Abeles, M. Predicting Movement from Multiunit Activity. *J. Neurosci.* **27**, 8387–8394 (2007).
- [68] Moran, A., Bergman, H., Israel, Z. & Bar-Gad, I. Subthalamic nucleus functional organization revealed by parkinsonian neuronal oscillations and synchrony. *Brain* **131**, 3395–3409 (2008).

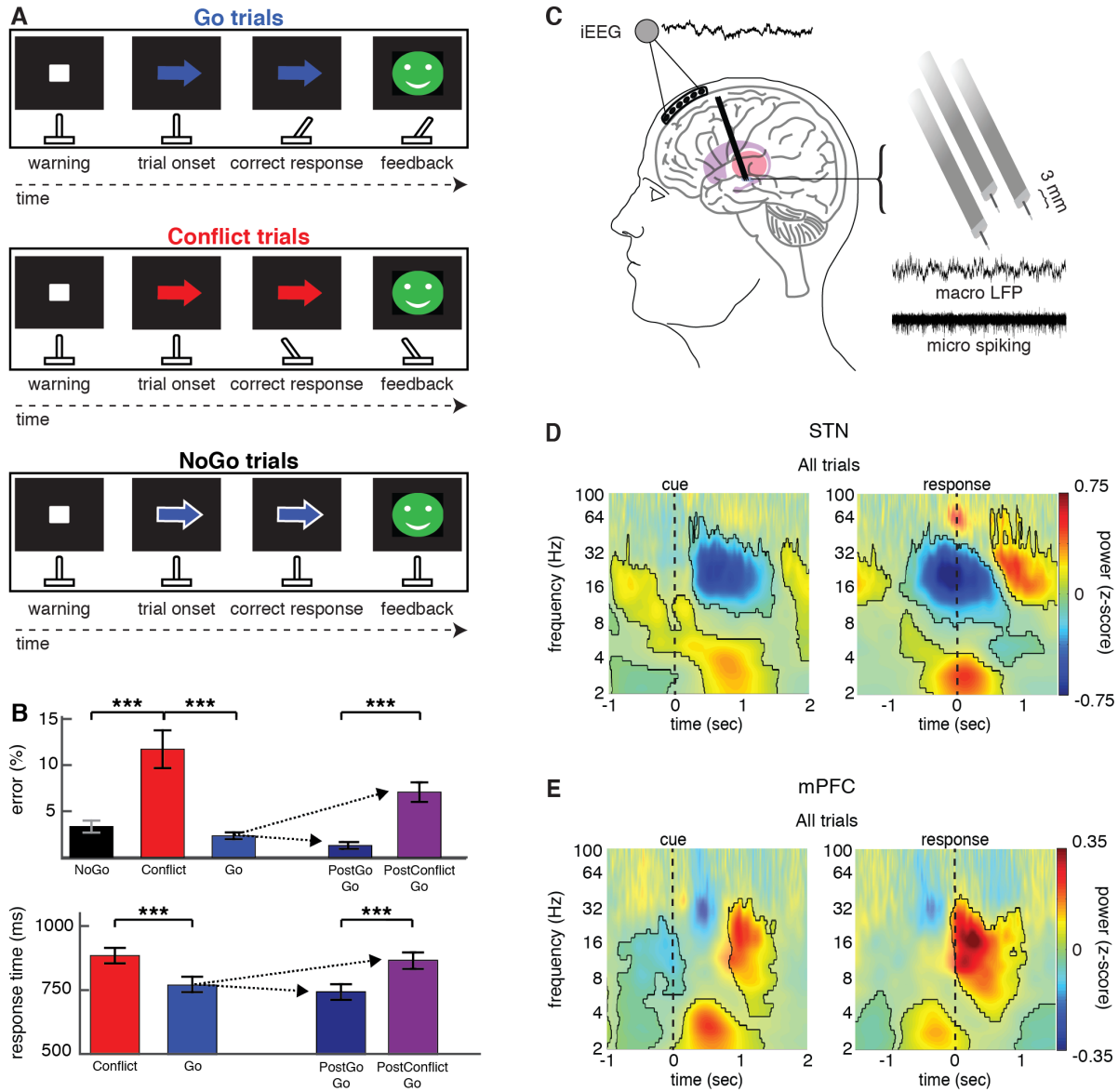


Figure 1 Arrow task during recordings captured from the human subthalamic nucleus (STN) and medial prefrontal cortex (mPFC). (A) Task. A warning cue appears on the screen to prepare the participant for the upcoming trial. During each trial, a colored arrow appears on the screen to indicate the appropriate action. If the arrow is blue, the participant must move a handheld joystick in the direction the arrow is pointing (Go trials). If the arrow is red, the movement must be in the opposite direction from where the arrow is pointing (Conflict trials). If the arrow has a white border around it (regardless of arrow color), the participant must withhold all movements (NoGo trials). (B) Error rates during the intraoperative sessions, averaged across participants (mean \pm SEM, $n=34$), are shown in the upper panel. Average response times during the correct trials are shown in the lower panel. Error rates and reaction times for all correct Go trials are also plotted separately for Go trials that followed a previous Go trial and Go trials that followed a Conflict trial. *** indicates $p < 0.001$. Overall, subjects showed higher error rates and slower reaction times during the Conflict trials. Go trials that followed a Conflict trial (PostConflict Go) also showed slower reaction times and higher error rates. (C) Six-contact electrode strips are placed over the mPFC to capture intracranial EEG activity during the task. Simultaneously, three macro/microelectrode pairs capture LFP (macro) and action potential spiking activity (micro) from the STN. A 5 s sample recording is shown for each. (D) Normalized oscillatory power averaged across all STN electrodes and across all correct trials. Data are aligned to arrow onset (left) and to the motor response (right, $t=0$); mask indicates time-frequency regions exhibiting significant differences from baseline at $p < 0.05$, corrected for multiple comparisons, permutation test. NoGo trials were excluded from the response aligned analysis. (E) Same as (D) but for the mPFC. Both brain regions showed a pre-response increase in theta power, although this is earlier and greatest averaged to the cue in the case of mPFC. In the beta band, the STN showed a pre-response decrease in power while the mPFC showed a post-response increase in beta power.

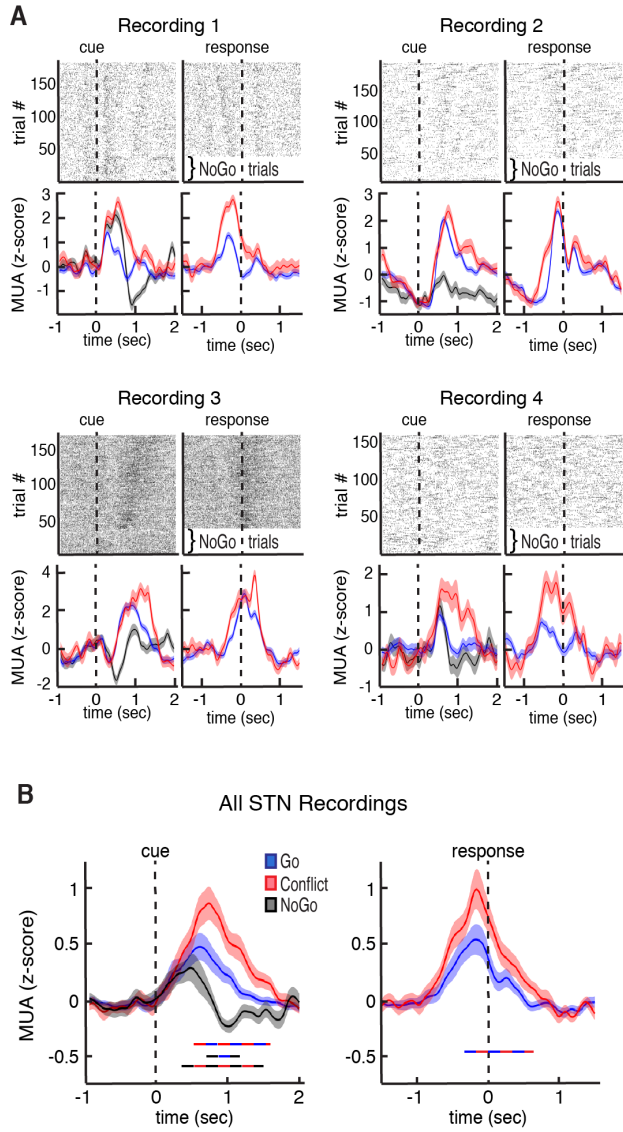


Figure 2 Task-related changes in multi unit activity in the STN. (A) Top: Raster plot for four neuronal clusters exhibiting changes in voltage thresholded spiking activity during the task. Bottom: Multiunit activity (MUA) was extracted from each recording and plotted separately for Go, Conflict, and NoGo trials. Data are aligned to arrow onset (left) and to the motor response (right, $t=0$) for four separate recordings. (B) Average continuous-time MUA for all STN microelectrode recordings that showed spiking activity. Time points exhibiting a significant difference between trial types ($p < 0.05$, corrected for multiple comparisons, permutation test) are denoted by colored horizontal bars denoting which comparison was made. Conflict trials showed significantly higher MUA than Go trials. Notably, the trials in which participants inhibited all movements (NoGo trials) showed the lowest average MUA levels.

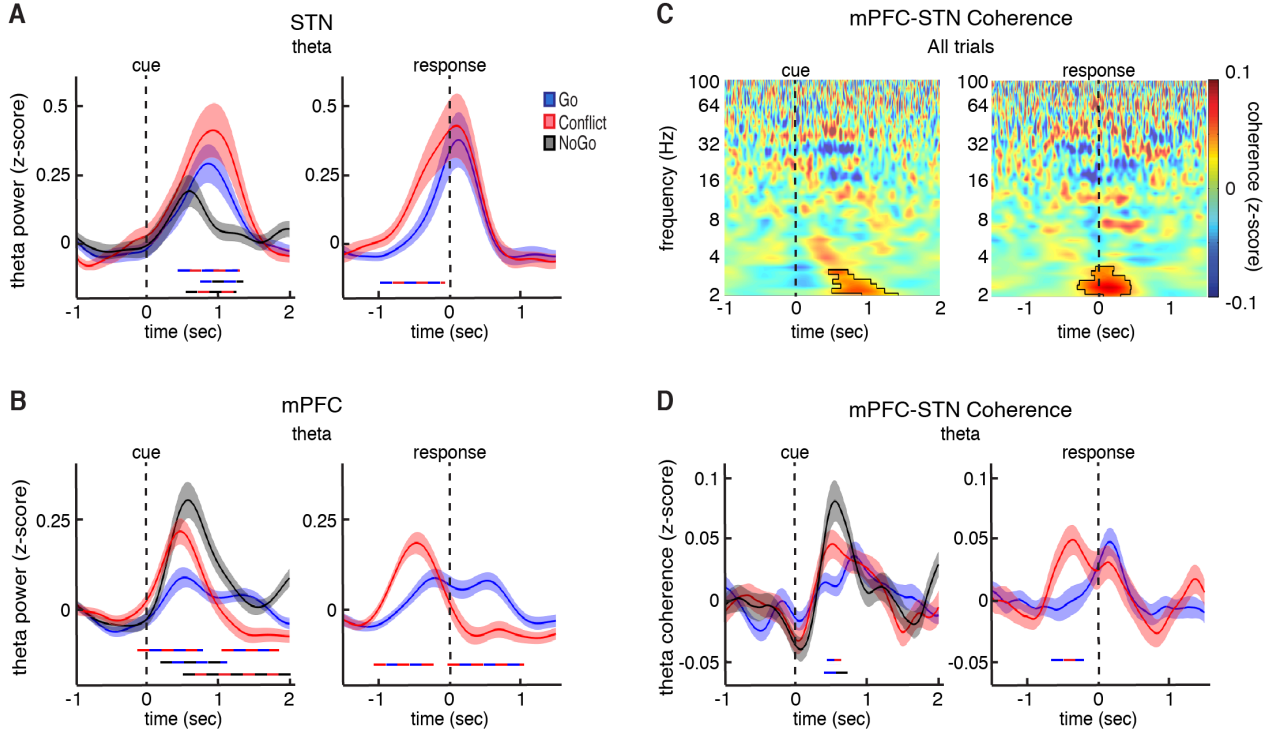


Figure 3 Trial type related differences in theta power and mPFC-STN phase coherence. (A) Cue and response aligned time evolving theta power changes averaged over all STN electrodes during the Go, Conflict, and NoGo trials. Time points exhibiting a significant difference between trial types ($p < 0.05$, corrected for multiple comparisons, permutation test) are denoted by colored horizontal bars denoting which comparison was made. (B) Same as (A) but for the mPFC. (C) Normalized mPFC-STN phase coherence averaged across all mPFC-STN electrode pairs and across all correct trials. Mask indicates time-frequency regions exhibiting significant differences from baseline at $p < 0.05$, corrected for multiple comparisons, permutation test. NoGo trials were excluded from the response aligned analysis. (D) Same data as (C) but averaged across the theta band and plotted separately for the Go, Conflict, and NoGo trials. Time points exhibiting a significant difference between trial types are denoted as in (A). In general, conflict and response inhibition involved higher levels of theta power and mPFC-STN phase coherence prior to the response.

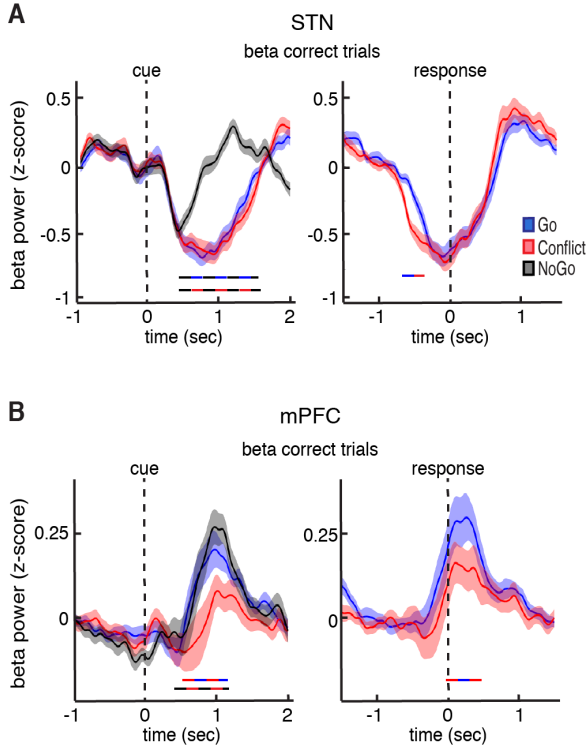


Figure 4 Trial type related differences in beta power. (A) Cue and response aligned time evolving beta power changes averaged over all STN electrodes during the Go, Conflict, and NoGo trials. Time points exhibiting a significant difference between trial types ($p < 0.05$, corrected for multiple comparisons, permutation test) are denoted by colored horizontal bars denoting which comparison was made. (B) Same as (A) but for the mPFC. Whereas the STN showed a pre-response decrease in beta power that was suppressed when movement had to be completely withheld, the mPFC showed a post-response increase in beta power that was suppressed during the more difficult Conflict trials.

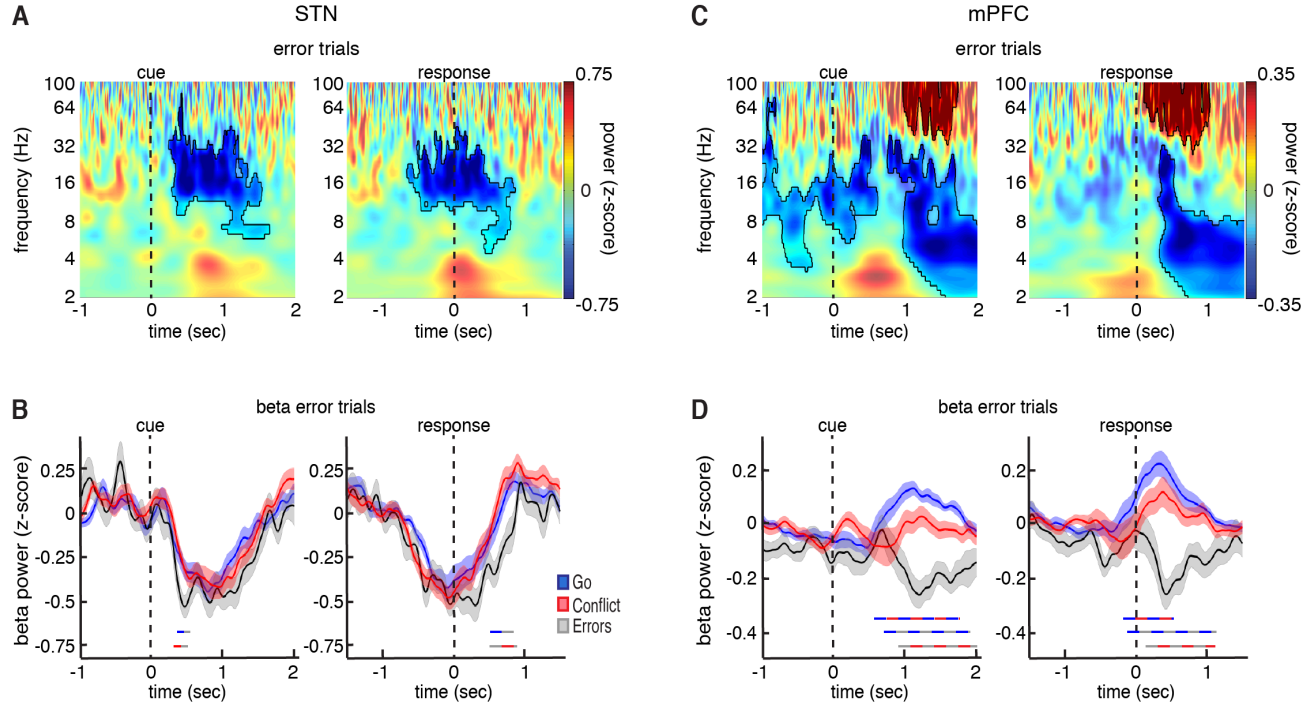


Figure 5 Trial type related differences in beta power during errors. (A) Normalized oscillatory power averaged across all STN electrodes and across all incorrect trials. Mask indicates time-frequency regions exhibiting significant differences from baseline at $p < 0.05$, corrected for multiple comparisons, permutation test. (B) Same as (A) but averaged across the entire beta band. The beta power time series are also shown for the Go and Conflict trials for comparison. Time points exhibiting a significant difference between trial types ($p < 0.05$, corrected for multiple comparisons, permutation test) are denoted by colored horizontal bars denoting which comparison was made. (C,D) Same as (A,B) but for the mPFC. Whereas the STN showed an early decrease in beta power that was more pronounced during error trials, the mPFC showed a post-response increase in beta power that was attenuated or even reversed during trials that involved either conflict or errors.

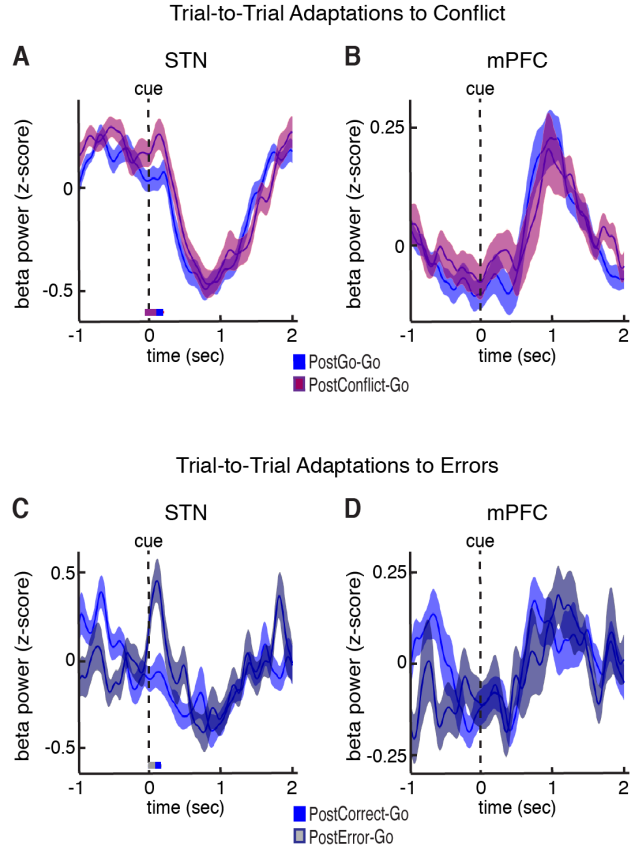


Figure 6 Changes in oscillatory power related to across-trial adaptations to conflict and errors. (A) Cue aligned time evolving beta power changes averaged over all STN electrodes during the correct Go trials that followed a correct Go trial (postGo-Go) and during the correct Go trials that followed a correct Conflict trial (postConflict-Go). Time points exhibiting a significant difference between trial types ($p < 0.05$, corrected for multiple comparisons, permutation test) are denoted by colored horizontal bars. (B) Same as (A) but for the mPFC. (C,D) Same as (A,B) but plotted for the correct Go trials that followed any correct trial (postCorrect-Go) and for the correct Go trials that followed any error trial (postError-Go). Only the STN showed a post-Conflict and post-error related increase in beta power right after the arrow presentation of the second trial.

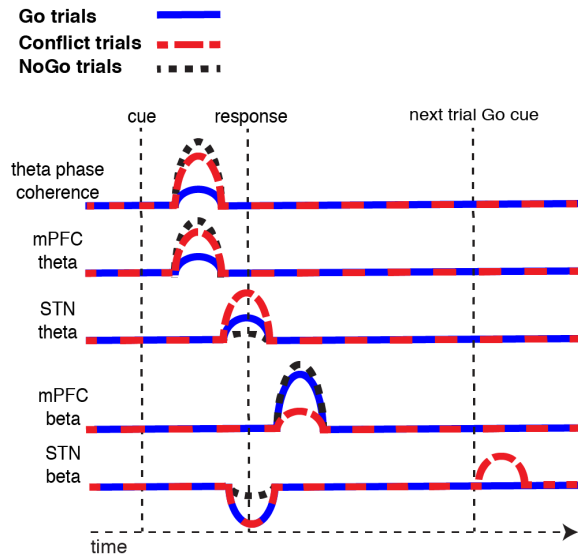


Figure 7 Summary schematic of trial type related differences. Following the presentation of the cue, mPFC-STN coherence and mPFC theta power increases, and this increase is significantly higher during Conflict and NoGo trials. Around the time of the response, STN theta power also increases, but this increase is only significantly higher during the Conflict trials and not the NoGo trials. The motor response is also associated with a decrease in STN beta power, and this decrease is attenuated during NoGo trials. Following each trial, there is an increase in mPFC beta power and this increase is attenuated during Conflict trials and during error trials (not shown). On a subsequent Go trial that follows a correct Conflict trial (or an error trial, not shown), there is an increase in STN beta power when the Go stimulus is presented.